IEEE Open Journal of Vehicular Technology

Received 17 December 2023; accepted 11 January 2024. Date of publication 16 January 2024;
date of current version 6 February 2024. The review of this article was coordinated by Editor Hongsheng Lu.

Digital Object Identifier 10.1109/OJVT.2024.3354393

CAI^{2}M^2: A Centralized Autonomous Inclusive Intersection Management Mechanism for Heterogeneous Connected Vehicles

ASHKAN GHOLAMHOSSEINIAN (Member, IEEE), AND JOCHEN SEITZ (Member, IEEE)

Communication Networks Group, Technische Universität, 98693 Ilmenau, Germany

CORRESPONDING AUTHOR: ASHKAN GHOLAMHOSSEINIAN (e-mail: ashkan.gholamhosseinian@tu-ilmenau.de)

This work was supported by the German Federal Ministry of Digital Affairs and Transport (BMDV) under Grant 45FGU138-A.

ABSTRACT This paper introduces a novel centralized autonomous inclusive intersection management mechanism (CAI^{2}M^2) for heterogeneous connected vehicles (HCVs). The system embraces a diverse array of human-driven vehicles, each possessing unique characteristics. The proposed system navigates vehicles through the intersection safely and efficiently considering various road conditions including dry (D), wet (W), snowy (S), and icy (I). The communication relies on dedicated short-range communications (DSRC) to facilitate the seamless exchange of traffic information between roadside unit (RSU) and vehicles. The coordination policy takes into account parameters such as vehicle types, arrival times, intersection rules, road priorities, and prevailing road conditions. To enhance safety and prevent collisions, vehicles are classified based on distinctive safety features and dynamics, such as reaction distance (d_r), stopping distance (d_s), braking distance (d_b), braking lag distance (d_{bl}), acceleration ($acc.$), deceleration ($dec.$), load, and velocity (v). The paper evaluates the system performance through metrics encompassing average travel time (ATT), packet loss rate (PLR), throughput, intersection busy time (IBT), and channel busy rate (CBR) across several traffic scenarios with different densities and distribution patterns. Additionally, the study compares the system efficiency with signalized intersections under various road conditions, aiming to identify an optimal control approach for autonomous intersection management

INDEX TERMS Heterogeneous connected vehicles, intersection management, ATT, CBR, PLR, IBT, throughput, coefficient of friction, road conditions, AIM.

I. INTRODUCTION

Connected vehicle technologies are shaping the future of transportation and land use on a global scale. They can dramatically enhance traffic safety, efficiency, comfort, and maximize the environmental sustainability, economic development, social well-being, and fleet management [1]. Roughly 26000 road casualties and one million road crashes with injuries were recorded in the European countries in 2015 [2]. In the road safety sector, intersections are well-established as one of the most critical spots for collisions. The U.S. department of transportation outlined that in the U.S. 28% of fatal crashes and 58% of nonfatal injuries occurred at intersections in 2019 leading to tremendous economic and societal costs [3].

Wireless vehicular communication is evolving rapidly primarily in wireless areas. Dedicated short-range communications (DSRC) [4] and ITS-G5 [5] are two radio technologies used for vehicular communications in the U.S. and Europe respectively. Nevertheless, the landscape has changed in the U.S. with the emergence of cellular vehicle-to-everything (C-V2X) technology, based on cellular networks (3G, 4G LTE, and later 5G). This standard has been introduced by the U.S. federal communications commission as an alternative and dominant solution that leverages existing cellular infrastructure for communication between vehicles and infrastructure incorporating several reformations and features.

Vehicle-to-infrastructure (V2I) and vehicle-to-vehicle (V2V) communications are known as two important deployment technologies of connected vehicles where vehicles communicate and share information with other vehicles or with nearby infrastructure. These emerging connectivity

models are anticipated to drive traffic management towards autonomy. It is expected that crashes on the road decline by 80% using V2I and V2V while reducing the travel delays [6]. Scientists have predicted that 20% and 80% of intersections will become V2I-enabled by 2025 and 2040 respectively [7]. It is also reported that 90% of light-duty vehicles will be capable of V2V communication by 2040 [7]. In this context, we must regard that vulnerable road users (VRUs) are exposed to high collision risks. Moreover, optimal trip time and speed at the intersection are other traffic concerns that call for an imminent consideration.

Vehicle classification (VC) is one of the major technologies for traffic management and monitoring [8]. It plays a vital role in traffic safety at the intersection. This is due to the diversity of different vehicles mobility and physical traits on the road that widely influence road safety [9]. For instance, velocity (v), vehicle load, acceleration ($acc.$), deceleration ($dec.$), and braking technology are distinctive key factors in the vehicle safety. In addition, road condition is recognized as an influential safety metric as the coefficient of friction (CoF) totally differs in various road conditions. It is worth noting that safety-related parameters are notably correlated.

In this study, we focus on developing and analyzing a framework for an autonomous intersection management (AIM) system, emphasizing its core functionalities and performance under various traffic scenarios. The proposed paper exploits CAI^{2}M^2 to convey a safe and efficient control mechanism at an autonomous intersection. The contributions of the paper are summarized as follows.

- *Enriched vehicle types:* In contrast to the majority of intersection management approaches in the literature that studied similar vehicles behaviour, we have highlighted the integration of heterogeneous connected vehicles (HCVs) on the road [10]. This research has expanded the scope of vehicle types by introducing trams, VRUs (bicycles, motorcycles, mopeds), delivery cars, heavy vehicles (trucks, semitrailers, trailers, buses, flexible buses, coaches), emergency vehicles (ambulance, police, fire-brigade), passenger vehicles (PVs) (van, sedan, hatchback, wagon), electric scooters (E-scooters), and electric-PVs (EPVs) [11], [12] into the system. This inclusion diversifies the vehicular landscape and better mirrors real-world traffic scenarios.
- *acc. inclusion:* Our previous works [13], [14] primarily examined the impact of different vehicle characteristics and dynamics of HCVs on intersection safety [10] at a basic level. In the current study, we have incorporated *acc.* into vehicle modeling and parameterization and rigorously assessed its influence on vehicle safety and dynamics, contributing to a more accurate representation of real-world traffic behaviors. Furthermore, we have explored the impact of the CoF on the ultimate vehicle *acc.*.
- *Enhanced system analysis:* While our earlier work [14] mainly considered the default (D) road condition in most of the results, this study delves into more complex and advance performance evaluation by interpolating the impact of various road conditions on the system performance. The system utilizes multiple metrics such as packet loss rate (PLR), intersection busy time (IBT), throughput, channel busy ratio (CBR) and average travel time (ATT) to provide a more holistic view of the system performance.
- Enhanced algorithm performance: Building upon our prior algorithmic framework in [14], we have refined and tuned its functionality to enhance its overall performance, accuracy, and responsiveness.
- Unlike our previous work [13], [14], the present study augments the influence of various road conditions in non-autonomous scenarios. Consequently, analogous to the autonomous intersection, traffic lights scenarios also encompass four different road conditions within both asymmetric and symmetric traffic. This enhancement enables us to more accurately estimate the impact of diverse road conditions on vehicle dynamics and safety.
- Akin to the principal methodology used in [13], [14], we utilize vehicular ad-hoc networks (VANETs) to classify vehicles with respect to the safety attributes of different vehicles [9]. The proposed system employs various road conditions such as dry (D), wet (W), snowy (S), and icy (I) as an underlying safety factor in the intersection management.

By explicitly outlining these distinctions, we aim to illustrate the evolutionary trajectory of our research. This new study not only builds upon our earlier groundwork but also introduces novel insights and improvements that contribute to a more comprehensive and advanced autonomous intersection system.

The remainder of paper is organized as follows. Section II introduces the latest works on AIM. Section III addresses the system model that entails radio technology, safety message parameters, and system operation. Section IV deals with vehicle modeling comprising vehicle parameters, type behavior and safety. The simulation platform and configuration settings are described in Section V. The performance evaluation including several metrics such as PLR, CBR, ATT, IBT and throughput is presented in Section VI. Finally, we conclude the paper and introduce the future work in Section VII.

II. RELATED WORK

In [10], we extensively covered AIM approaches in a systematic way. Here, we build upon our former study to introduce some of the latest research efforts conducted on AIM thereafter. State of the art embodies a wide range of methods that are usually formulated as optimization problems or machine learning methods.

Wen et al. [15] addressed connected vehicle speed control in urban areas using V2I and V2V communications. It introduced a hierarchical scheme for platoon-road control, ensuring traffic flow balance and stability through intersection managers and an integral sliding mode controller. Authors

in [16] proposed a sustainable connected autonomous vehicles CAVs system architecture for roundabout crossings. It utilized V2I communication to manage vehicle behavior and traffic flow, aiming for energy efficiency and safety. The central signaling unit coordinated vehicle movements through a block-based reservation policy. In another effort [17], an autonomous vehicle control method using V2I and V2V communications was explored. The system analyzed model predictive control (MPC) for intersection coordination. The proposed method achieved similar travel times to offline optimization, making it more applicable in real traffic scenarios due to reduced energy consumption. Abbas-Turki et al. [18] investigated intersection management using inter-vehicular communication. It highlighted the customization of vehicle speed and scheduling based on traffic demand using distributed particle swarm optimization. The study employed flow-speed diagrams to assess optimization impact on traffic engineering. Similar work using MPC was presented in [19] where they deployed a safe, scalable, and robust hierarchical AIM system. This system involved two layers: a global centralized layer where an infrastructure allocated safe speeds to vehicles to minimize system cost, and a local decentralized layer where vehicles used their sensors to follow assigned speeds, avoid collisions, and make independent movement decisions.

Researchers in [20] discussed a decentralized strategy for managing CAVs at signal-free intersections, considering uncertainties and energy efficiency using a hierarchical robust control approach. Simulation results showed its efficacy to reach a trade-off between energy consumption and travel time. In [21], a novel scheme was developed to optimize the vehicle passages in high traffic loads by integrating Monte Carlo tree search strategy and grouping cooperative approach. Furthermore, the study [22] addressed the centralized coordination of CAVs by employing a hierarchical convex optimal protocol to minimize energy consumption and travel time. Cong et al. [23] constructed a safe distributed cooperative AIM framework for CAVs utilizing multiple virtual platoons. In another work, Chen et al. [24] utilized a safe cooperative grouping control technique in addition to a Petri net model to navigate CAVs through unsignalized intersections with lower fuel consumption. In [25], a collaborative turning point decision framework for mixed traffic was introduced to enhance traffic efficiency and safety at intersections via a central manager. In addition, the work [26] proposed a safe and efficient distributed decision-making method for mixed traffic at non-signalized intersections. In addition, several works in literature attempted to use mixed-integer linear programming (MILP). For example, [27] benefited from advantages of different intersection modeling approaches to optimize the CAVs crossing with V2V and V2I communications using MILP. Likewise, the study [28] exploited an intersection control system using dynamic programming and MILP that took advantage of CAVs as traffic regulators in a mixed traffic environment. Further, safe centralized approaches for coordination of CAVs were presented in [29], [30], [31] as prevalent intersection control solution to improve traffic efficiency.

There are several scholars that have contributed to the AIM using various machine learning methods. For example, Lombard et al. [32] proposed a novel reinforcement learning (RL) approach using V2V and V2I communications to optimize right-of-way distribution. RL outperformed traffic lights and the classic first-come first-serve (FCFS) cooperative method, increasing traffic flow and reducing emissions. Huang et al. [33] worked on a centralized RL-based methodology to schedule the maneuvers of CAVs at unsignalized intersections. Similarly, [34] introduced a multi-agent RL-based AIM system using continuous action space modeling and a self-attention proximal policy optimization algorithm. Moreover, Antonio et al. [35] developed a cooperative multi-agent decentralized RL method to provide safety and more efficiency for CAVs with respect to the traffic lights management. Authors in [36], [37], [38] harnessed the power of RL and graph neural networks (GNNs) to control mixed traffic at a collaborative multi-agent intersection planning framework, aiming to improve throughput and delay. In another scientific effort, Zheng et al. [39] studied a safe decentralized coordination system for CAVs using a combination of two multi-agent RL algorithms to alleviate efficiency and comfort at the non-signalized intersection. Additionally, Yan et al. [40] proposed an RL-based control method for mixed traffic at unsignalized three-way intersections for flow optimization. In a different approach [41], INTEL-PLT, an adaptive platoon-based autonomous intersection control model was assessed. It employed RL to optimize efficiency, fairness, and energy savings for CAVs. INTEL-PLT benefited from a two-level structure, combining a reservation-based policy with a deep Q-network algorithm to determine platoon size based on real-time traffic conditions.

It should be noted that the focus of most of the works in the literature revolves around mathematical modeling of simple intersections not considering DSRC, road conditions and VC. On the contrary, our work presented here has attempted to consider a novel and more complex intersection in terms of communication technology, heterogeneity of vehicles, road conditions, and vehicle distinct characteristics in a realist simulation using platforms that are well- tailored for vehicular communications to closely mimic DSRC functionalities and traffic behavior.

III. SYSTEM MODEL

Fig. 1 depicts an autonomous intersection in an urban environment where HCVs cross the unsignalized intersection without deployment of traffic lights. Bicycles and E-scooters have dedicated lanes. In contrast to the north-south road (NS) that only allows vehicle crossing, east-west road (EW) accommodates tram tracks traveling two-ways between west and east side of the intersection. A road side unit (RSU) schedules the vehicles crossing via V2I communication. In the context of intersection modeling, as discussed in [10],

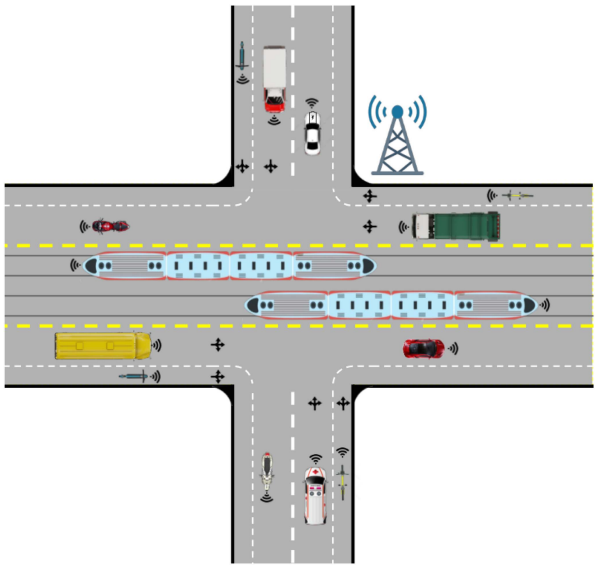

FIGURE 1. Intersection layout.

spatio-temporal reservation and trajectory planning are two distinct approaches with unique characteristics. The spatio-temporal reservation approach involves discretizing the intersection into grid cells, allowing vehicles to reserve specific cells along their paths for a designated time period. This method emphasizes cooperative resource scheduling. On the other hand, trajectory planning involves pre-defining travel paths for vehicles as they navigate through intersections, resulting in the identification of collision points. Both approaches can be implemented centrally or in a distributed manner. In this study, we have adopted the trajectory planning mechanism.

A. RADIO TECHNOLOGY

DSRC has been designed to excel in vehicular communications, offering low latency even in fast-paced and dynamic vehicular environments. It designates seven channels within the frequency range of 5.850–5.925 GHz [4], [42]. DSRC effectively utilizes the IEEE 802.11p standard at the physical layer, incorporating diverse transmission rates to enhance its performance [4], [42]. Medium access control (MAC) operation conforms to carrier sense multiple access/collision avoidance (CSMA/CA). Moreover, enhanced distributed channel access (EDCA) describes the degree of quality of service for a certain application. Highest level of EDCA, AC_VO, is assigned for safety applications [13], [14], [43]. The IEEE 1609.4 standard enables concurrent multichannel operation for DSRC [4]. Channel 178 acts as Control Channel (CCH) and deals with safety messages. Service Channels (SCHs) like channel number 174 are assigned for various kinds of services.

B. SAFETY MESSAGE PARAMETERS

1) MESSAGE TYPES

Our system employs two kinds of messages; the V2I message (V2IM) is disseminated from vehicle to the RSU encompassing kinematic and physical vehicular information. Vice versa, the I2V message (I2VM) is broadcast from the RSU to all nearby vehicles containing a list of allowed-to-pass vehicles. A warning message (WM) is timely triggered locally in vehicles that are not allowed to cross the intersection.

2) MESSAGE FORMAT

IEEE 1609.3 standard defines the WAVE (Wireless Access in Vehicular Environment) short message protocol (WSMP) in the network and transport layers of DSRC [44]. A bidirectional data exchange exists between the application layer and WSMP WSMP transmits WAVE short messages (WSM) to the receiver containing various information [44]. Here, we extend the WSM message to incorporate desired vehicular information in V2IM and I2VM from the application layer.

3) MESSAGE SIZE

The system adopts considerably small packet sizes of 138 and 10 bytes for V2IM and I2VM respectively to mitigate channel congestion and improve connection robustness.

C. SYSTEM OPERATION

Vehicles transmit V2IM encompassing both kinematic and physical attributes to the RSU. The RSU undertakes the task of orchestrating the incoming vehicles by first arranging them based on FCFS policy and their arrival times. Subsequently, a process of prioritization unfolds, influenced by several criteria such as direction priority (straight, right, left), road ranking, vehicle types, and more. As a result, a packet is disseminated to the vehicles, containing the list of authorized vehicles permitted to cross the intersection. The system utilizes two distinct states: the "Intersection-In" state, indicative of vehicles either nearing or traversing the intersection, and the "Intersection-Out" state, denoting vehicles that have successfully navigated through the intersection. These states are generated and embedded in the packets that are transmitted by vehicles to the RSU. Further, they particularly pertain to the spatial location of the vehicles as they navigate the intersection. For vehicles not meeting the criteria for passage, a WM is triggered to alert them, subsequently enabling them to stop according to their stopping distance. This mechanism ensures that vehicles with superior priority can traverse the intersection in a safe and efficient manner. Simultaneous right turns and opposite left turns are allowed.

In order to elevate the system performance and minimize the travel time, a concurrency mechanism allows vehicles with lower passing priority to pass through the intersection in parallel to the vehicles bearing the higher-ranked direction. This implies that a left turning vehicle can only cross the intersection with other vehicles if its trajectory does not collide with straight-going and also right turning vehicles. Likewise, right turning vehicles take into account straight-going vehicles for concurrent crossing. Furthermore, in case vehicles with similar passing priority on all roads jointly arrive

at the intersection, systems breaks the tie by letting vehicles on the EW to firstly drive through the intersection. It is worth mentioning that vehicles cross the intersection with maximum $acc.$. Algorithms 1 and 2 represent the RSU operation when it receives and transmits V2IM and I2VM from and to the vehicles respectively.

Algorithm 1: RSU Receiving State.

Input: V2IM including vehicle ID, vehicle type, time, road ID, lane ID, direction, and position
Output: List of allowed vehicle IDs
Initialize RSU database
while *vehicle position* ≡ *Intersection-In* ***and*** *RSU database is not empty* **do**
  Add or update vehicle data in RSU database
  Sort vehicles in RSU database based on FCFS policy
  Identify vehicles with the same arrival time
  forall $vehicles\ in\ RSU\ database$ **do**
    if $Direction \equiv Straight$ **then**
      Prioritize vehicles for straight crossing using CAI²M² based on vehicle type, road priority and right of way rules
      Add prioritized vehicles IDs to the list of allowed vehicles IDs
      forall $vehicles\ in\ RSU\ database$ **do**
        if $Direction \equiv Right$ ***and*** *its future trajectory does not conflict with the straight traveling vehicles* **then**
          Add $vehicle$ ID to the list of allowed vehicles IDs
        end
      end
      forall $vehicles\ in\ RSU\ database$ **do**
        if $Direction \equiv Left$ ***and*** *its future trajectory does not conflict with the straight and right-turning vehicles* **then**
          Add $vehicle$ ID to the list of allowed vehicles IDs
        end
      end
    end
    else if $Direction \equiv Right$ **then**
      Allow all vehicles to cross the intersection
      forall $vehicles\ in\ RSU\ database$ **do**
        if $Direction \equiv Left$ ***and*** *its future trajectory does not conflict with right-turning vehicles* **then**
          Add $vehicle$ ID to the list of allowed vehicles IDs
        end
      end
    end
    Prioritize left-turning vehicles using CAI²M²
    Add prioritized vehicles IDs to the list of allowed vehicle IDs
  end
end
Remove processed vehicles from RSU database

IV. VEHICLE MODELING

A. VEHICLE PARAMETERS

Enforcement of concrete road safety approaches stipulates that vehicles characteristics are distinct, and therefore they behave differently on the roads. In this context, we implement VC as it plays a pivotal role in the traffic management by retrieving multiple mobility and physical information from the vehicles [8]. In our previous work [9], we classified HCVs based on their safety-related properties using vehicular networks. The proposed system benefits from VC to ensure safety at the intersection. Here, stopping distance (d_s) of the vehicle is computed by means of braking distance (d_b), braking-lag distance (d_{bl}), reaction distance (d_r), reaction time (t_r) and braking-lag time (t_{bl}) [9], [14], [43]. Vehicles kinematic parameters significantly impact the aforementioned safety metrics. In addition, the system accounts for different road conditions such as D, W, S, and I. Drivers pavement surface results in various CoF that can drastically impact d_b and d_s. As such, road condition is a critical ingredient in timely vehicle braking.

B. VEHICLE TYPE BEHAVIOUR

Trams have the highest passing priority and can drive nonstop. They are passive in the conflict resolution and do not participate in the traffic management. Vehicles passage is adapted according to the arrival time of the tram. Emergency vehicles like police, ambulance and fire-brigade only yield to trams. The vehicles mobility model follows the intelligent driver model (IDM) [45] (as defined for Veins, cf. Section V). IDM is a popular choice for simulating realistic and accurate real-world traffic conditions as it takes into account human driving behavior, such as maintaining a safe following distance and adjusting speed based on the distance to the vehicle in front. The warning system considers a t_r of 1 s (s) [46] to warn the driver after the WM is shown [9]. Furthermore, vehicles constantly compute their d_s as they approach the intersection. As a result, the driver is notified to initiate braking and betimes stop at the intersection when the distance to the intersection reaches the d_s. The local warning system embedded in vehicles strengthens the reliability and decreases the computation effort on the RSU. Algorithms 3 and 4 explain the vehicle operation when it receives and sends I2VM and V2IM from and to the RSU respectively.

C. VEHICLE SAFETY

1) COEFFICIENT OF FRICTION (COF)

CoF is a measure of grip or traction between the vehicle tires and the road surface. The value is represented with μ and depends on various factors such as type of the road surface, tire type, weather conditions, etc. A higher value of μ leads to better grip, and hence higher dec. Furthermore, with higher CoF e.g. in the D roads, tires can transfer more traction and torque to the road surface, resulting in higher acc. Conversely, in lower CoF such as W, S, and I road conditions, tires have less grip on the road surface which can lead to lower $acc.$ and poor handling. It should be emphasized that other factors such as weight, slope of the road, rolling and air resistance can also affect $acc.$ and dec. Basically, CoF tends to higher values in the D pavement compared to W, S and I surfaces. Authors in [9] investigated an extensive research on CoF in

Algorithm 2: RSU Sending State.

Input: List of allowed vehicle IDs
Output: I2VM
Create and populate I2VM by setting vehicle IDs in the I2VM
Broadcast I2VM every second

different road conditions. They inferred to CoF of the D, W, S, and I road conditions as 0.77, 0.54, 0.21, and 0.08 respectively. Generally, rolling resistance is typically higher and more important in vehicle handling and performance on snow than on other road conditions. This is due to the depth, type density and texture of snow as well as skidding influence that can greatly impact the rolling resistance. When a vehicle drives over snow, snow can compact under the weight of the vehicle, causing the tires to sink into the snow and experience greater deformation. This can increase the rolling resistance of the tires and require more energy to move the vehicle forward, resulting in a higher rolling resistance. Therefore, to avoid rolling resistance computation, we have assumed that the snow depth is quite low in the existing work.

2) TIRE LOAD IMPACT (TLI)

TLI refers to the way a tire performance and characteristics can be affected by changes in the load or weight it is supporting. Specifically, it describes how a tire handling, traction, and wear characteristics can change as the load on the tire changes. It is an important consideration for vehicle manufacturers and drivers, as it can affect both safety and performance of the vehicle. TLI intimates that CoF is largely influenced by vehicle load, especially for heavy vehicles leading to longer d_b [9], [14], [43]. In reference to the friction theory, horizontal force is commensurate with the vertical load that is charged on tires. Nonetheless, in reality, tires do not adhere to this theory especially in terms of higher vertical loads. As such, the lateral force grows with slower pace than vertical load advancements [47]. For example, a trailer with 20,000 kg can only produce 16,000 kg lateral force, that is 0.8 g force [47]. Equation (1) proposes the the braking force f_b with respect to the TLI impact. Consequently, CoF with respect to the load can be derived for a heavy vehicle where *mass* and $mass_0$ [9] define the mass of the heavy vehicle in a loaded and empty status. μ_{TLI} corresponds to the CoF of the loaded vehicle while μ states the CoF in an ideal condition. Additionally, exponent $\alpha = 0.8$ is emanated from the concept of 0.8 g TLI force that was formerly discussed. The TLI does not impact trams as they never stop during the simulation. The system takes advantage of the TLI coefficient denoted as TLIC to acquire the final CoF [9].

$$\begin{aligned} F_b &= \mu_{(D,W,S,I)} mass_0 g \\ &= \mu_{TLI(D,W,S,I)} mass_0 g \left(\frac{mass}{mass_0}\right)^{\alpha} \end{aligned} \tag{1}$$

Algorithm 3: Vehicle Receiving State.

Input: I2VM
Output: Vehicle position
Initialize vehicle position
if *vehicle position* $\equiv$ $intersection - In$ ***and*** *vehicle ID* $\equiv$ *one of the allowed-to-go vehicles in the I2VM* **then**
  Cross the intersection with the maximum allowed acc.
  Update the vehicle position as $Intersection - Out$
else
  if *vehicle position* $\equiv$ $Intersection - In$ ***and*** $d_i \leq d_s$ **then**
    WM notifies the vehicle to stop
    Vehicle brakes and safely stops at the intersection
    Update the position of the vehicle as $Intersection - In$
  else
    Vehicle continues driving non stop
    Update the vehicle position as $Intersection - In$
  end
end

Algorithm 4: Vehicle Sending State.

Input: Vehicle state (ID, type, velocity, time, road ID, lane ID, direction, and position)
Output: V2IM
Calculate distance to the intersection (d_i)
Calculate vehicle direction
Calculate vehicle stopping time and d_s with respect to the vehicle safety-related parameters and current road condition
Create and populate V2IM
Broadcast V2IM with 10 Hz frequency

In (1), by replacing $\frac{1}{\left(\frac{mass}{mass_0}\right)^{\alpha}}$ with TLIC, we come to the (2) where we can conclude the final CoF incorporating the load impact.

$$\mu_{TLI(D,W,S,I)} = \frac{\mu_{(D,W,S,I)}}{\left(\frac{mass}{mass_0}\right)^{\alpha}} = TLIC \cdot \mu_{(D,W,S,I)} \tag{2}$$

3) DECELERATION (*dec.*)

Maximum $dec.$, namely ($dec._{\max}$) of the typical vehicle, e.g, VRUs, PVs or EPVs in different road conditions such as D, W, S, and I is measured as the product of CoF of the specific road pavement with respect to the load namely $\mu_{TLI(\mathrm{D,\,W,\,S,\,I})}$ and gravitational $acc.$ of g as shown in (3). Load does not incur any impact on μ of the light vehicles. Thus, $dec._{\max}$ of the light vehicles is computed in (4) wherein $\mu_{TLI(\mathrm{D,\,W,\,S,\,I})}$ equals the primary μ in different road conditions denoted as $\mu_{(D,W,S,I)}$.

$$dec._{\max} = -\mu_{TLI(\mathrm{D,\,W,\,S,\,I})} \cdot g \tag{3}$$

$$dec._{VRUS/PV/EPVs} = -\mu_{TLI(\mathrm{D,\,W,\,S,\,I})} \cdot g = -\mu_{(\mathrm{D,\,W,\,S,\,I})} \cdot g \tag{4}$$

On the other hand, based on the TLI (1), load impacts the actual CoF of heavy vehicles differently as shown in Table 1. The impact of snow depth on $dec._{\max}$ can be significant. It

TABLE 1. Vehicle Parameters

Vehicle Type	$v\ (km/h)$	$acc._{initial}\ (m/s^2)$	$acc._{(D,\,W,\,S,\,I)}\ (m/s^2)$	$dec._{(D,\,W,\,S,\,I)}\ (m/s^2)$	$\mu_{TLI(D,\,W,\,S,\,I)}$	$TLIC$	$t_{bl}\ (s)$	$t_r\ (s)$	$mass(tons)$	$mass_0(tons)$
Bike	20	1.2	1.2, 0.84, 0.32, 0.12,	7.55, 5.30, 2.06, 0.78	0.77, 0.54, 0.21, 0.08	1	0	1	-	-
E-scooter	25	4.0	4.0, 2.8, 1.08, 0.4,	7.55, 5.30, 2.06, 0.78	0.77, 0.54, 0.21, 0.08	1	0	1	-	-
Moped	40	1.1	1.1, 0.77 0.30, 0.11	7.55, 5.30, 2.06, 0.78	0.77, 0.54, 0.21, 0.08	1	0	1	-	-
Motorcycle	50	6.0	6.0, 4.2 1.62, 0.6	7.55, 5.30, 2.06, 0.78	0.77, 0.54, 0.21, 0.08	1	0	1	-	-
PVs	50	2.6	2.6, 1.82 0.70, 0.26	7.55, 5.30, 2.06, 0.78	0.77, 0.54, 0.21, 0.08	1	0.1	1	-	-
EPVs	50	3.9	3.9, 2.73 1.05, 0.39	7.55, 5.30, 2.06, 0.78	0.77, 0.54, 0.21, 0.08	1	0.1	1	-	-
Ambulance	100	2.6	2.6, 1.82 0.70, 0.26	7.55, 5.30, 2.06, 0.78	0.77, 0.54, 0.21, 0.08	1	0.1	1	-	-
Police	100	2.6	2.6, 1.82 0.70, 0.26	7.55, 5.30, 2.06, 0.78	0.77, 0.54, 0.21, 0.08	1	0.1	1	-	-
Fire-brigade	100	1.3	0.74, 0.52 0.20, 0.08	4.30, 3.02, 1.17, 0.44	0.44, 0.31, 0.12, 0.05	0.57	0.4	1	-	-
Delivery	50	2.6	1.69, 1.18 0.46, 0.17	4.91, 3.45, 1.34, 0.51	0.50, 0.35, 0.14, 0.05	0.65	0.1	1	8.5	5
Truck	50	1.3	0.74, 0.52 0.20, 0.08	4.30, 3.02, 1.17, 0.44	0.44, 0.31, 0.12, 0.05	0.57	0.4	1	30	15
Semitrailer	50	1.1	0.55, 0.38 0.15, 0.06	3.77, 2.65, 1.03, 0.39	0.38, 0.27, 0.10, 0.04	0.50	0.4	1	40	17
Trailer	50	1.0	0.41, 0.29 0.11, 0.04	3.10, 2.17, 0.84, 0.32	0.32, 0.22, 0.09, 0.03	0.41	0.4	1	60	20
Bus	50	1.2	1.03, 0.72 0.28, 0.11	6.49, 4.56, 1.77, 0.67	0.66, 0.46, 0.18, 0.07	0.86	0.4	1	14.5	12
Flexible Bus	50	1.2	1.01, 0.71 0.27, 0.10	6.34, 4.45, 1.73, 0.65	0.65, 0.45, 0.18, 0.07	0.84	0.4	1	21	17
Couch Bus	50	2.0	1.50, 1.05 0.41, 0.15	5.66, 3.98, 1.55, 0.58	0.58, 0.40, 0.16, 0.06	0.75	0.4	1	17	12
Tram	50	1.0	0.72, 0.50 0.20, 0.07	5.44, 3.82, 1.48, 0.56	0.55, 0.39, 0.15, 0.06	0.72	0.4	1	60	40

is influenced by various factors including density, type and texture of the snow, vehicle-specific features and tire characteristics. Snow depth affects the rolling resistance, traction, grip and interaction between the tires and the road surface, ultimately influencing the maximum $dec.$ of the vehicle. To this end, in this study, we assume that snow depth is minimal thereby, impact of snow depth is negligible. $dec.$ of different heavy vehicles considering the load impact are computed in (5), (6), (7), and (8).

$$dec._{\text{Delivery}} = -0.65 \cdot dec._{\max} \tag{5}$$

$$dec._{(Truck/Fire-brigade/Semitrailer/Trailer)} = -(0.57/0.57/0.50/0.41) \cdot dec._{\max} \tag{6}$$

$$dec._{(bus/Flexible-bus/Coach)} = -(0.86/0.84/0.75) \cdot dec._{\max} \tag{7}$$

$$dec._{Tram} = -0.72 \cdot dec._{\max} \tag{8}$$

4) ACCELERATION ($acc.$)

In addition to $dec.$, $acc.$ of a vehicle alters under different road conditions. This value remains unchanged for the light vehicles in different road conditions whereas in terms of the heavy vehicles, the final $acc.$ is affected by the TLI factor depending on the load of the vehicle. $acc.$ of a vehicle based on the initial $acc.$ ($acc._{initial}$) in all other road conditions, $acc._{(D,W,S,I)}$, is calculated in (9) where $\mu_{TLI(D,W,S,I)}$ represents the CoF of the D, W, S, I roads considering the TLI

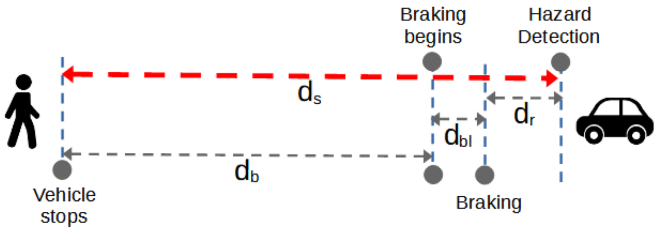

FIGURE 2. Stopping distance components.

impact, and μ_D indicates the CoF in a D surface condition.

$$acc._{(D,W,S,I)} = \frac{\mu_{TLI(D,W,S,I)}}{\mu_{(D)}} \cdot acc._{initial} \tag{9}$$

5) STOPPING DISTANCE (d_s)

d_s is the total distance a vehicle moves from the time the vehicle recognizes a hazard to the moment the vehicle comes to a complete stop. d_s is formulated as the aggregation of d_r, d_b and d_{bl} as described in (10). Fig. 2 illustrates the components of the d_s.

$$d_s = d_r + d_{bl} + d_b \tag{10}$$

6) REACTION DISTANCE (d_r)

d_r is the distance a vehicle drives from the moment a vehicle recognizes a hazard to the time it begins to apply the brakes, or take evasive action to avoid the hazard. d_r is influenced by driver's decision-making and perception (reaction time t_r), and vehicle speed. Equation (11) indicates the d_r. The value "3.6" represents the conversion factor from kilometers per hour (km/h) to meters per second (m/s).

$$d_r = \frac{v}{3.6} \cdot t_r \tag{11}$$

7) BRAKING DISTANCE (d_b)

Braking distance is the distance a vehicle travels from the moment the braking begins until the vehicle comes to a complete stop. Equation (12) argues that d_b of the vehicles depends on $dec.$ which is the multiplication of CoF with parameter μ and gravitational $acc.$ as g with the value of 9.81 m/s^2 [9].

$$d_b = \frac{\left(\frac{v}{3.6}\right)^2}{-2 \cdot dec._{\max}} \tag{12}$$

8) BRAKING-LAG DISTANCE (d_{bl})

d_{bl} is the distance a vehicle covers from the moment the brakes are applied until the brakes respond and vehicle starts to decelerate. Vehicle weight, speed and braking system determine the d_{bl}. Braking lag time (t_{bl}) implicates the time that vehicle braking system requires to reach the equilibrium state. Braking technology is different in heavy and light vehicles leading to various t_{bl}. t_{bl} of 0.1 s pertains to light trucks and ordinary vehicles whereas it drops to 0.4 s for heavy vehicles [9]. Equation (13) demonstrates the d_{bl}.

$$d_{bl} = \frac{v}{3.6} \cdot t_{bl} \tag{13}$$

TABLE 2. Vehicles Traveling Plan in Asymmetric Traffic Scenarios

Road	Total	Straight	Right turn	Left turn
EW	8	4	2	2
NS	4	2	1	1
EW	16	8	4	4
NS	8	4	2	2
EW	24	12	6	6
NS	12	4	4	4
EW	32	16	8	8
NS	16	8	4	4

TABLE 3. Vehicles Traveling Plan in Symmetric Traffic Scenarios

Road	Total	Straight	Right turn	Left turn
EW	6	2	2	2
NS	6	2	2	2
EW	12	4	4	4
NS	12	4	4	4
EW	18	6	6	6
NS	18	6	6	6
EW	24	8	8	8
NS	24	8	8	8

V. SIMULATION

We have adopted vehicles in network simulation (Veins) [48] that bidirectionally couples two simulation platforms via transmission control protocol (TCP) link. Objective modular network testbed in C++ (OMNeT++) [49] performs as a wireless network simulator, and simulation of urban mobility (SUMO) [50] as a traffic simulator. Table 1 shows the vehicles modeling parameters including physical, mobility and safety attributes. In order to examine the system performance in an autonomous intersection scenario under realistic condition, default collision-free settings are discarded in SUMO. Eight sparse and congested traffic scenarios with asymmetric and symmetric flows are designed to assess the performance of the system in different road conditions of the autonomous intersection. A symmetric flow copes with even distribution of inbound vehicles on the four legs of the junction such that the outbound flow also conforms to this paradigm. On the contrary, in the asymmetric flow, vehicles mostly prefer EW for traveling on the entrance and exit roads to the intersection. The vehicles traveling plans in the asymmetric and symmetric flows are shown in Tables 2 and 3 respectively. Moreover, we compare the system results to the conventional traffic lights control (TLC).

Sparse traffic scenarios host 12 and 24 veh/km^2 while congested scenarios entails 36 and 48 veh/km^2. By including a range of density values, from sparse to dense, we allow a thorough examination of how different levels of vehicle

concentration impact system behavior, congestion patterns, and overall efficiency. In the first sparse scenario with 12 veh/km^2 we have encapsulated all 11 main categories of vehicle types including tram, bike, E-scooters, moped, motorcycle, PVs, EPVs, emergency vehicle, delivery, truck, and bus. We recognize the importance of considering different types of vehicles within these scenarios. To achieve this, we have carefully managed the inclusion of vehicle types, especially as traffic density increases. As density increases to 24, 36 and 48 veh/km^2, diversity of vehicles elevates such that system can include more vehicles sub-types. For instance, additional classes of buses such as coach and flexible bus, various sub-types of emergency vehicles comprising police, fire-brigade, and police, and auxiliary truck classes such as semi-trailer, and trailer can also contribute to the network. This strategy guarantees a wider variety of vehicle types to avoid repetition and ensure a more realistic and representative sample. Moreover, distribution of the vehicles is modeled in a way that every entrance road holds different vehicle types. We have refrained from interpolation of similar vehicles on the same road as much as possible. Our intention was to replicate scenarios that reflect common actual traffic conditions while also aligning with the focus of our study.

Vehicles drive in the simulation area with the maximum v and travel with 50 km/h. This is a common speed in an urban environment. Emergency vehicles disobey this rule as they can travel with 100 km/h on all roads. Moped, bicycles and E-scooters speed are set to 40, 25 and 20 km/h respectively. Table 4 summarizes the simulation parameters.

To compare the performance of the proposed system with the signalized intersection, we devise an optimal TLC planning. To this end, in addition to the vehicles, bicycle lanes are also controlled by the TLC to enable safe and efficient movement of cyclists and E-scooters through the intersection. All vehicles with green light should perpetually yield to the trams as they have the highest right of way. 36 s and 12 s are planned as the green phase duration of vehicle and cyclist lanes in the asymmetric traffic respectively [51]. Furthermore, the system adjusts 24 s and 8 s for the green phase of the vehicles and bicycle lanes on the NS road respectively [51]. On the other hand, the system avails 36 s for the all vehicles lanes and 12 s for whole bicycle lanes as the green phase in the symmetric traffic [51]. Traffic lights operation in the asymmetric and symmetric streams are illustrated in Figs. 3 and 4 respectively.

TABLE 4. Simulation Settings

Simulation Parameters	Value
Vehicle beacon rate	10 Hz
RSU beacon rate	1 Hz
RSU height	5 m
Channel No.	CCH (178), SCH (174)
Access layer protocol	DSRC
Radio frequency	5.9 GHz
Data rate	6 $Mbps$
MAC model	IEEE 1609.4
Networking/transport model	IEEE 1609.3
PHY model	IEEE 802.11p
Transmit power	20 mW
I2VM and V2IM size	10, 138 $bytes$
Path loss model	Free space
Road length	4 × 400 m
Vehicle density	12, 24, 36, 48 veh/km^2
Car-following model	IDM
Asymmetric TLC green lights for EW	36 s (vehicle lanes) 12 s (bicycle lanes)
Asymmetric TLC green lights for NS	24 s (vehicle lanes) 8 s (bicycle lanes)
Symmetric TLC green lights	36 s (EW/NS)
$\mu_{(D,W,S,I)}$	0.77, 0.54, 0.21, 0.08

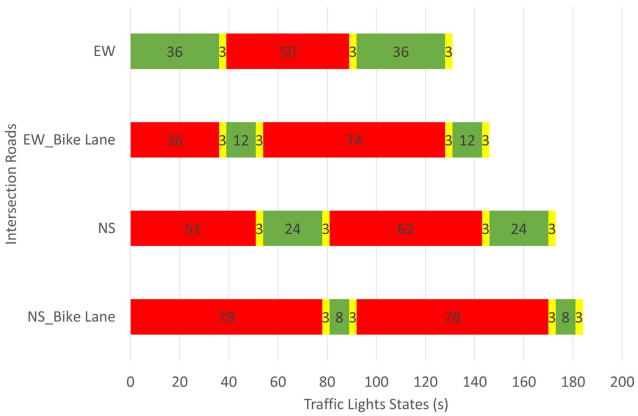

FIGURE 3. Traffic lights phases in asymmetric traffic.

VI. PERFORMANCE EVALUATION

We benefit from several metrics to estimate the system performance in diverse traffic conditions as mentioned below.

A. PACKET LOSS RATE (PLR)

Safe and reliable V2I communication greatly depends on the packet success ratio of the vehicles and RSU. Packet loss occurs due to signal fading, collisions, or channel congestion [52]. Channel congestion potentially happens in dense networks with a large number of packet transmissions. Basically, the system measures PLR for RSU and n number of vehicles as shown in (14).

$$PLR = \sum_{i=1}^{n} \frac{\text{Number of lost packets}}{\text{Total number of sent packets}} \cdot 100\% \qquad (14)$$

Figs. 5 and 6 depict the percentage of RSU and vehicles PLR in several traffic densities from 12-asymmetric (12-A) to 48-A in conjunction with 12-symmetric (12-S) to 48-S. Totally, PLR is remarkably trivial for vehicles and RSU in different scenarios. PLR of the RSU demonstrate 0.5% as

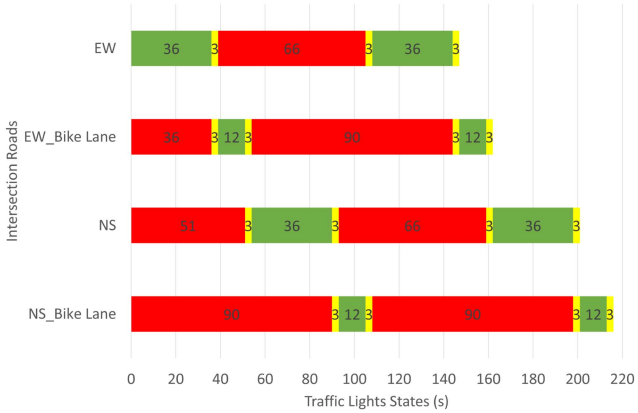

FIGURE 4. Traffic lights phases in symmetric traffic.

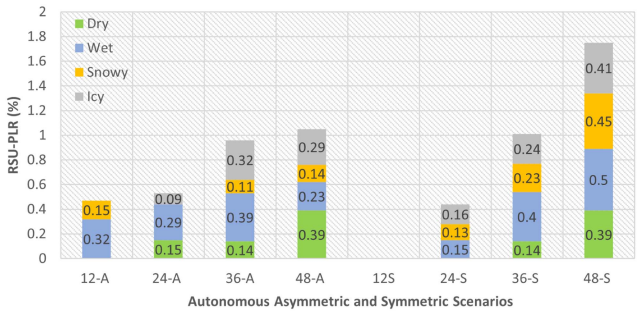

FIGURE 5. PLR of the RSU in the autonomous scenarios.

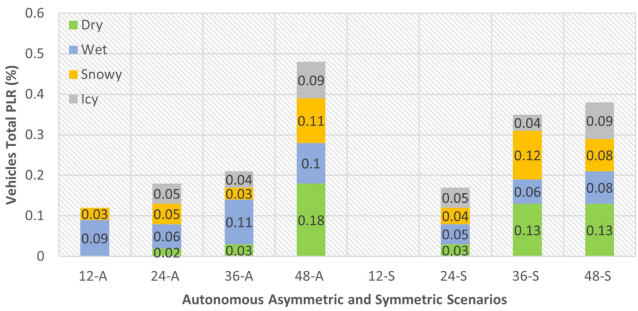

FIGURE 6. Total PLR of vehicles in the autonomous scenarios.

the maximum point in the entire road conditions with 12-S Veh/km^2 vehicle density and 0% as the minimum value in the W road with 48-S Veh/km^2 scenario. W road has shown to produce the most PLR in more than 60% of the scenarios. Moreover, the figure indicates the negative effect of congestion on PLR where in all scenarios total PLR increases together with the traffic density expansion. Similar to the PLR behaviour in the RSU, all 12-S scenarios succeeded to deliver all the packets to the RSU. On the other hand, 48-A veh/km^2 on the *D* road released the highest PLR among all scenarios by 0.18%. Like the PLR performance in the RSU figure, total vehicles PLR is proportional to the vehicular density. All in all, these results manifest that the system is quite dependable and can deliver safety packets with high accuracy.

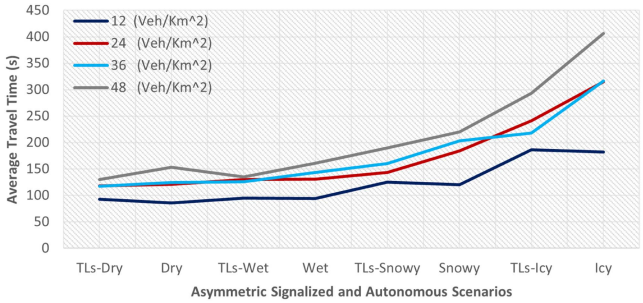

FIGURE 7. ATT in asymmetric traffic.

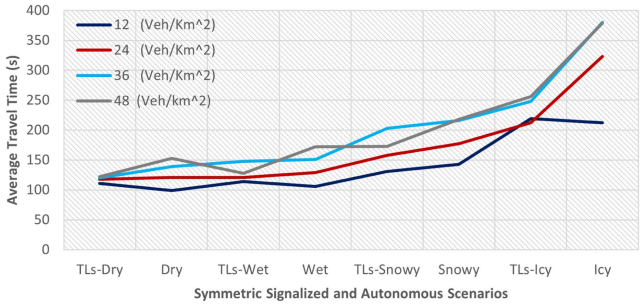

FIGURE 8. ATT in symmetric traffic.

B. AVERAGE TRAVEL TIME (ATT)

Fig. 7 denotes the vehicles ATT in 8 autonomous and non-autonomous asymmetric traffic scenarios. Vehicles in 12 veh/km^2 flow experienced nearly 8, 4 and 2% less ATT in the D, S and I roads compared to the signalized traffic scenarios respectively. Besides, vehicles traveled with marginally lower ATT on the W road in the autonomous scenario. The traffic density of 24 veh/km^2 showed slightly better performance for the D road in the autonomous intersection and uniform output for the W roads in both TLC and autonomous scenarios in terms of ATT. In contrast, vehicles in the S and I roads encountered longer travel time by roughly 30% in a non-signalized intersection. In the event of 36 veh/km^2, autonomous junction with the D road could approximately maintain a comparable ATT to the TLC scenario, while by switching to the W, S and I conditions vehicles ATT rocketed by 10, 20 and 30% respectively. Relating to the 48 veh/km^2, ATT raised by around 15% in both D and W roads in the autonomous intersection. This value rose to about 14% in the autonomous S road condition before climbing gradually to almost 28% in the I road.

Fig. 8 shows the ATT of vehicles in 8 autonomous and non-autonomous symmetric traffic scenarios. The comparison of symmetric and asymmetric figures for 12 veh/km^2 represents that ATT of autonomous intersection increased by 4% in the D, S roads and 1% on the I road in the symmetric scenarios. Moreover, W road illustrated a sharp growth by 8% compared to the equivalent case in the asymmetric scenario. Information on 24 veh/km^2 enumerates that ATT in the D road is

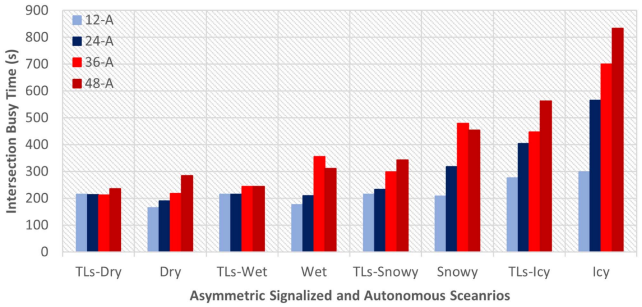

FIGURE 9. IBT in autonomous asymmetric scenarios.

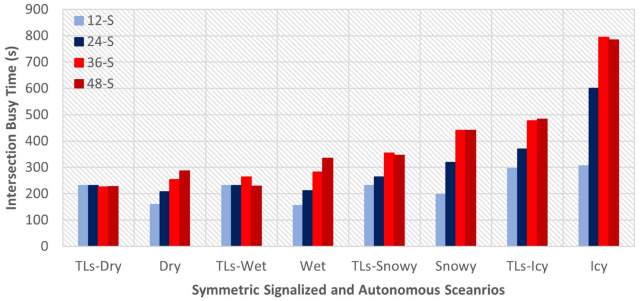

FIGURE 10. IBT in autonomous symmetric scenarios.

moderately stabilized for the D and W road conditions in both TLC and autonomous cases. Conversely, by switching from autonomous to the TLC, ATT slowly upsurged close to 11% and 34% in S and I roads. Data on 36 veh/km^2 describes that ATT of the D and I roads in the autonomous crossroad went up by 14% and 35% while it leveled off for the W road condition. Furthermore, S road ATT experience a modest increase by moving from the TLC to the autonomous case by 6%. With regard to the 48 veh/km^2, the trend of ATT delineates that it soared from the TLC to the autonomous D and S roads by 20%. In addition, it depicted that autonomous W and I roads dropped behind the TLC by 25 and 32% respectively.

Basically, both ATT figures express a considerable contrast between 36 and 48 veh/km^2 in the S and I roads of the signalized and autonomous intersections. In the signalized intersection on the S and I road conditions, road participants especially heavy vehicles accelerate and maneuver very slowly at the intersection. As a result, some vehicles might no be able to pass through the intersection before the TLC switches to green for the other vehicles. This causes a chaotic and hazardous situation where several vehicles are in the middle of the intersection trying to cross simultaneously. As opposed to this problem that potentially occurs in the signalized junction, autonomous intersection strictly avoids such a dilemma by safely navigating the vehicles through intersection leading to more ATT.

C. INTERSECTION BUSY TIME (IBT)

Fig. 9 outlines the IBT of autonomous and signalized intersection scenarios in the asymmetric traffic. The figure summarizes that by automating the intersection, IBT of 12-A declined by 23%, 18% and 4% in the D, W and S roads respectively. Even in the I road, the autonomous intersection could certainly match the TLC performance. In the 24-A, autonomous scenarios outperformed the TLC in the D and W roads by 11% and 2% respectively. Further, autonomous S and I roads exhibited 36% and 40% more IBT than non-autonomous scenarios. IBT yielded faintly higher outcome in 36-A of the D road in autonomous scenario whilst the efficiency deteriorated ranging from 31% to 38% in the following autonomous scenarios against the TLC scenarios. Additionally, in terms of 48-A scenario, IBT of the D, W, S and I roads

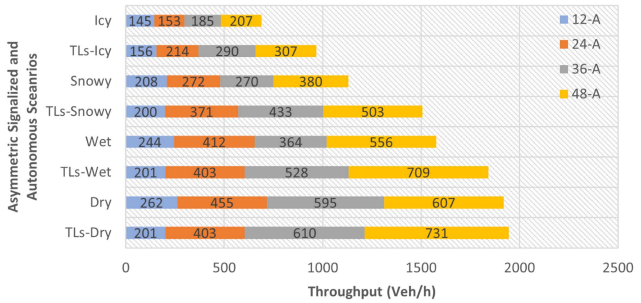

FIGURE 11. Intersection throughput in autonomous asymmetric scenarios.

with the TLC surpassed autonomous counterparts by 21%, 27%, 33%, and 48% respectively.

Fig. 10 sketches out the IBT of autonomous and signalized intersection scenarios in the symmetric traffic. Results demonstrate that by using autonomous intersection in 12-S scenario, IBT plummeted by nearly 31% for the D and 33% for the W roads. Furthermore, IBT disparity with the autonomous cases decreased by 16% and 29% in the S and I roads. Moreover, IBT of 24-S in the autonomous D and W scenarios improved by almost 10%. Adversely, S and I roads provided worse IBT than the TLC by 17% and 38% respectively. Referring to 36-S, moving from the TLC to non-signalized intersection resulted in 12%, 7%, 25%, and 66% higher IBT in the D, W, S and I scenarios receptively. Concerning 48-S in the D, W, S and I roads, IBT showed better results for the TLC by 26%, 46%, 27%, and 62% respectively.

D. INTERSECTION THROUGHPUT

Fig. 11 presents throughput in different signalized and autonomous asymmetric scenarios. It is evident that the autonomous D, W, S scenarios in 12-A vehicle per square kilometer performed better than their rivals in the signalized intersection. In addition, the I road scenario acquired a throughput close to the TLC-icy scenario. Supremacy of the autonomous D and W scenarios over the TLC continued in 24-A traffic density while throughput of the TLC-snowy and the TLC-icy scenarios excelled the corresponding values in the autonomous intersection. In addition, the signalized intersection appeared to be more efficient than the autonomous one in terms of throughput in all road types of 36-A and 48-A

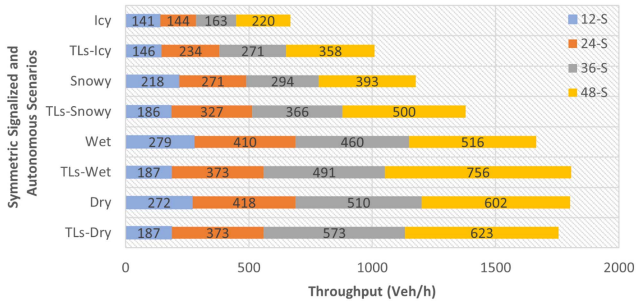

FIGURE 12. Intersection throughput in autonomous symmetric scenarios.

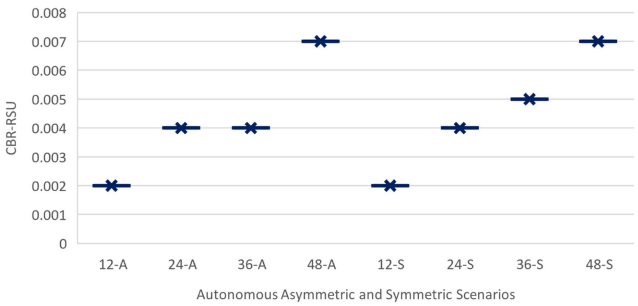

FIGURE 13. CBR of RSU in autonomous scenarios.

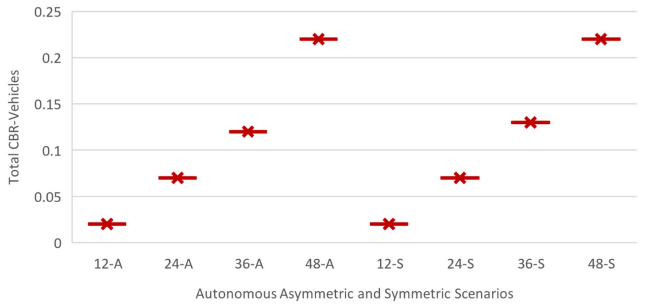

FIGURE 14. Vehicles CBR in autonomous scenarios.

vehicles densities. As mentioned before, the reason lies in the CoF impact on the movement of the vehicles at the TLC thereby, a situation might occur where multiple vehicles from different directions try to cross the intersection at the same time. The more the traffic is congested, the more difference between throughput of the TLC and autonomous scenario is probable to happen. Fig. 12 explains the proportion of the throughput in the autonomous scenarios to the TLC. Here, throughput resembles the behavior of the asymmetric traffic shown in Fig. 11.

E. CHANNEL BUSY RATE (CBR)

Vehicular networks are burdened with restricted channel bandwidth which is shared among road entities such as RSU and vehicles. It is worth noting that successful packet delivery without latency or loss is highly dependant on the channel congestion, especially in dense areas [52]. Furthermore, saturated wireless channel has an adverse impact on transmission range [52]. CBR specifies the the ratio of channel busy time to the whole observation time, e.g, 100 ms. CBR relies on the packet size, traffic density and transmission rate. Besides, it is recognized as one of the underlying facets of PLR [52], [53]. Equation (15) refers to CBR where $t_{busy,i}$, t_{total}, n stand for channel busy duration, total simulation time and number of vehicles respectively [54].

$$CBR = \sum_{i=1}^{n} \frac{t_{busy,i}}{t_{total}} \tag{15}$$

Figs. 13 and 14 reflect the RSU and vehicles total CBR in the non-signalized intersection. Fig. 14 shows relatively analogous CBR in the symmetric and asymmetric flows in 12, 24 and 48 veh/km^2. Furthermore, symmetric traffic with 36 veh/km^2 gained somewhat higher CBR in comparison to the same traffic density in the symmetric flow. Furthermore, CBR for the RSU experienced a comparable behavior in both symmetric and asymmetric cases except for the 36 veh/km^2 where CBR of symmetric traffic escalated by 25% compared to the asymmetric traffic. As a whole, the system was competent to maintain the channel load to a minor level for vehicles and RSU leading to a reliable communication.

VII. CONCLUSION AND FUTURE WORK

This paper attempted to propose an inclusive safe AIM scheme for HCVs using V2I communication. We exploited VC to classify vehicles considering several safety parameters and pavement surface conditions. We also adopted PLR and CBR to analyze the communication safety. In addition, we sought to provide efficiency at the intersection by enhancing ATT, throughput, and IBT. A wide range of scenarios was conducted in terms of traffic density, traffic load distribution and road conditions. The implementation part discussed about the extension of the DSRC protocol to insert proprietary vehicular information in the safety messages of vehicles and RSU. We developed a warning mechanism to timely warn the human-driven vehicles with inferior priorities to stop at the intersection. Evaluation results asserted that the proposed system is capable of establishing safety with minimal PLR and CBR. Besides, ATT of all autonomous asymmetric scenarios in the least congested traffic density manifested more efficiency than the TLC. Furthermore, in the 24-A scenario, the D and W autonomous cases gained parallel ATT to the TLC scenarios. Even in the the 36-A D road scenario, autonomous scenario achieved almost homogeneous ATT to the TLC. ATT in autonomous symmetric traffic achieved equal results to the TLC for D and W roads in 24-S while they performed more efficient than the corresponding values in the 12-S TLC scenario. The system also gained an ATT in the 24-S D that was moderately comparable to the TLC. Apart from autonomous 12-S S case, 12-S autonomous I scenario also outperformed the TLC. As regards to throughput and IBT in asymmetric and symmetric traffic, we witnessed the comparable performance as the ATT figures.

The measurement of d_s and the presence of WM on every individual vehicle removes computational overhead from the RSU such that it can handle the intersection management with more permanence and durability. Additionally, compared to the distributed approach, our centralized model promotes the communication range and reduces the collision likelihood. Moreover, V2I approach can complement the vehicle sensor-based safety systems by improving the vehicle perception and vision. In future, we plan to investigate the effect of different V2I propagation models and weather conditions on the signal quality.

REFERENCES

[1] A. Nikitas, I. Kougias, E. Alyavina, and E. N. Tchouamou, "How can autonomous and connected vehicles, electromobility, brt, hyperloop, shared use mobility and mobility-as-a-service shape transport futures for the context of smart cities?," *Urban Sci.*, vol. 1, no. 4, 2017, Art. no. 36. [Online]. Available: https://www.mdpi.com/2413-8851/1/4/36

[2] "The future of road transport, implications of automated, connected, low-carbon and shared mobility," *Eur. Commission, Joint Res. Centre,* Ispra, Italy, Tech. Rep. EUR 29748 EN, Apr. 2019.

[3] L. Blincoe et al., "The economic and societal impact of motor vehicle crashes, 2019," *Nat. Highway Traffic Saf. Admin. (NHTSA)*, Washington, DC, USA, Tech. Rep. DOT HS 813 403, Dec. 2022.

[4] F. Arena, G. Pau, and A. Severino, "A review on IEEE 802.11p for intelligent transportation systems," *J. Sensor Actuator Netw.*, vol. 9, no. 2, 2020, Art. no. 22. [Online]. Available: https://www.mdpi.com/2224-2708/9/2/22

[5] A. Gholamhosseinian and J. Seitz, "Empirical estimation of ETSI ITS-G5 performance over an IPv6-based platform," in *Proc. IEEE Int. Perform. Comput. Commun. Conf.*, 2022, pp. 185–193.

[6] U.S. Department of Transportation, "Planning for the future of transportation: Connected vehicles and ITS" ITS Joint Program Office, Technical Report, FHWA-JPO-15-214, 2015.

[7] E. P. Dennis, P. E. A. Spulber, V. S. Brugeman, R. Kuntzsch, and R. Neuner, "Planning for connected and automated vehicles," *Center Automot. Res. Public Sector Consultants*, Lansing and Ann Arbor, Michigan, Mar. 2017. [Online]. Available: https://www.cargroup.org/wp-content/uploads/2017/03/Planning-for-Connected-and-Automated-Vehicles-Report.pdf

[8] A. Gholamhosseinian and J. Seitz, "Vehicle classification in intelligent transport systems: An overview, methods and software perspective," *IEEE Open J. Intell. Transp. Syst.*, vol. 2, pp. 173–194, 2021.

[9] A. Gholamhosseinian and J. Seitz, "Safety-centric vehicle classification using vehicular networks," in *Proc. 16th Int. Conf. Future Netw. Commun.*, 2021, pp. 238–245.

[10] A. Gholamhosseinian and J. Seitz, "A comprehensive survey on cooperative intersection management for heterogeneous connected vehicles," *IEEE Access*, vol. 10, pp. 7937–7972, 2022.

[11] Electric vehicle database, "Acceleration of full electric vehicles," Nov. 2023. [Online]. Available: https://ev-database.org/cheatsheet/acceleration-electric-car

[12] Tomas Zajicek, "Fastest accelerating electric cars 0-100 km/h," myEVreview, Sep. 2023. [Online]. Available: https://www.myevreview.com/fastest-accelerating-electric-cars-0-100

[13] A. Gholamhosseinian and J. Seitz, "Plenary autonomous intersection management protocol for heterogeneous connected vehicles," in *Proc. 14th Int. Conf. Ubiquitous Future Netw.*, 2023, pp. 334–336.

[14] A. Gholamhosseinian and J. Seitz, "PCIMS: Plenary centralized intersection management scheme for heterogeneous connected vehicles," in *Proc. IEEE Int. Conf. Omni-Layer Intell. Syst.*, 2023, pp. 1–6.

[15] S. Wen and G. Guo, "Control of connected vehicles in road network via traffic flow information feedback," *IEEE Trans. Intell. Transp. Syst.*, vol. 24, no. 12, pp. 14267–14280, Dec. 2023.

[16] L. Hota, B. P. Nayak, A. Kumar, B. Sahoo, and G. G. M. N. Ali, "A performance analysis of VANETs propagation models and routing protocols," *Sustainability*, vol. 14, no. 3, 2022, Art. no. 1379. [Online]. Available: https://www.mdpi.com/2071-1050/14/3/1379

[17] Z. Farkas, A. Mihály, and P. Gáspár, "Analysis of model predictive intersection control for autonomous vehicles," *Periodica Polytechnica Transp. Eng.*, vol. 51, no. 3, pp. 209–215, 2023. [Online]. Available: https://pp.bme.hu/tr/article/view/22082

[18] A. Abbas-Turki et al., "Autonomous intersection management: Optimal trajectories and efficient scheduling," *Sensors*, vol. 23, no. 3, 2023, Art. no. 1509. [Online]. Available: https://www.mdpi.com/1424-8220/23/3/1509

[19] S. Chamideh, W. Tärneberg, and M. Kihl, "A safe and robust autonomous intersection management system using a hierarchical control strategy and V2I communication," *IEEE Syst. J.*, vol. 17, no. 1, pp. 50–61, Mar. 2023.

[20] X. Pan, B. Chen, L. Dai, S. Timotheou, and S. A. Evangelou, "A hierarchical robust control strategy for decentralized signal-free intersection management," *IEEE Trans. Control Syst. Technol.*, vol. 31, no. 5, pp. 2011–2026, Sep. 2023.

[21] J. Peng, W. Wang, S. Zou, and G. Wang, "An efficient collaborative framework for connected and automated vehicles at unsignalized intersections under various traffic loads," in *Proc. 6th CAA Int. Conf. Veh. Control Intell.*, 2022, pp. 1–6.

[22] X. Pan, B. Chen, S. Timotheou, and S. A. Evangelou, "A convex optimal control framework for autonomous vehicle intersection crossing," *IEEE Trans. Intell. Transp. Syst.*, vol. 24, no. 1, pp. 163–177, Jan. 2023.

[23] X. Cong, B. Yang, F. Gao, C. Chen, and Y. Tang, "Virtual platoon based CAVs cooperative driving at unsignalized intersection," in *Proc. IEEE 25th Int. Conf. Intell. Transp. Syst.*, 2022, pp. 53–58.

[24] C. Chen, B. Wu, L. Xuan, J. Chen, and L. Qian, "A discrete control method for the unsignalized intersection based on cooperative grouping," *IEEE Trans. Veh. Technol.*, vol. 71, no. 1, pp. 123–136, Jan. 2022.

[25] S. Li, K. Shu, Y. Zhou, D. Cao, and B. Ran, "Cooperative critical turning point-based decision-making and planning for CAVH intersection management system," *IEEE Trans. Intell. Transp. Syst.*, vol. 23, no. 8, pp. 11062–11072, Aug. 2022.

[26] F. Yang and Y. Shen, "Distributed scheduling at non-signalized intersections with mixed cooperative and non-cooperative vehicles," *IEEE Trans. Veh. Technol.*, vol. 72, no. 6, pp. 7123–7136, Jun. 2023.

[27] Z. Yao, H. Jiang, Y. Jiang, and B. Ran, "A two-stage optimization method for schedule and trajectory of CAVs at an isolated autonomous intersection," *IEEE Trans. Intell. Transp. Syst.*, vol. 24, no. 3, pp. 3263–3281, Mar. 2023.

[28] P.-C. Chen, X. Liu, C.-W. Lin, C. Huang, and Q. Zhu, "Mixed-traffic intersection management utilizing connected and autonomous vehicles as traffic regulators," in *Proc. 28th Asia South Pacific Des. Automat. Conf.*, 2023, pp. 52–57.

[29] C. Vitale, P. Kolios, and G. Ellinas, "Optimizing vehicle reordering events in coordinated autonomous intersection crossings under CAVs' location uncertainty," *IEEE Trans. Intell. Veh.*, vol. 8, no. 5, pp. 3473–3488, May 2023.

[30] J. Rouyer, A. Ninet, H. Fouchal, and A. Keziou, "A road intersection control in urban intelligent transportation systems," in *Proc. IEEE Int. Conf. Commun.*, 2022, pp. 3562–3567.

[31] A. Hadjigeorgiou and S. Timotheou, "Real-time optimization of fuel-consumption and travel-time of CAVs for cooperative intersection crossing," *IEEE Trans. Intell. Veh.*, vol. 8, no. 1, pp. 313–329, Jan. 2023.

[32] A. Lombard, A. Noubli, A. Abbas-Turki, N. Gaud, and S. Galland, "Deep reinforcement learning approach for V2X managed intersections of connected vehicles," *IEEE Trans. Intell. Transp. Syst.*, vol. 24, no. 7, pp. 7178–7189, Jul. 2023.

[33] S.-C. Huang, K.-E. Lin, C.-Y. Kuo, L.-H. Lin, M. O. Sayin, and C.-W. Lin, "Reinforcement-learning-based job-shop scheduling for intelligent intersection management," in *Proc. Des. Automat. Test Eur. Conf. Exhib.*, 2023, pp. 1–6.

[34] J. Xue, B. Li, and R. Zhang, "Multi-agent reinforcement learning-based autonomous intersection management protocol with attention mechanism," in *Proc. IEEE 25th Int. Conf. Comput. Supported Cooperative Work Des.*, 2022, pp. 1132–1137.

[35] G.-P. Antonio and C. Maria-Dolores, "Multi-agent deep reinforcement learning to manage connected autonomous vehicles at tomorrow's intersections," *IEEE Trans. Veh. Technol.*, vol. 71, no. 7, pp. 7033–7043, Jul. 2022.

[36] M. Klimke, J. Gerigk, B. Völz, and M. Buchholz, "An enhanced graph representation for machine learning based automatic intersection management," in *Proc. IEEE 25th Int. Conf. Intell. Transp. Syst.*, 2022, pp. 523–530.

[37] M. Klimke, B. Völz, and M. Buchholz, "Automatic intersection management in mixed traffic using reinforcement learning and graph neural networks," in *Proc. IEEE Intell. Veh. Symp. (IV)*, 2023, pp. 1–8.
[38] M. Klimke, B. Völz, and M. Buchholz, "Cooperative behavior planning for automated driving using graph neural networks," in *Proc. IEEE Intell. Veh. Symp. (IV)*, 2022, pp. 167–174.
[39] J. Zheng, K. Zhu, and R. Wang, "Deep reinforcement learning for autonomous vehicles collaboration at unsignalized intersections," in *Proc. IEEE Glob. Commun. Conf.*, 2022, pp. 1115–1120.
[40] S. Yan, T. Welschehold, D. Büscher, and W. Burgard, "Courteous behavior of automated vehicles at unsignalized intersections via reinforcement learning," *IEEE Robot. Automat. Lett.*, vol. 7, no. 1, pp. 191–198, Jan. 2022.
[41] D. Li, J. Wu, F. Zhu, T. Chen, and Y. D. Wong, "Modeling adaptive platoon and reservation-based intersection control for connected and autonomous vehicles employing deep reinforcement learning," *Comput.-Aided Civil Infrastructure Eng.*, vol. 38, no. 10, pp. 1346–1364, Dec. 2022, doi: 10.1111/mice.12956.
[42] A. Izadi, A. Gholamhosseinian, and J. Seitz, "Vanet-based traffic light management for an emergency vehicle," in *Ubiquitous Networking*. Berlin, Germany: Springer, 2023, pp. 129–137.
[43] A. Gholamhosseinian and J. Seitz, "Versatile safe autonomous intersection management protocol for heterogeneous connected vehicles," in *Proc. IEEE Veh. Power Propulsion Conf.*, 2022, pp. 1–7.
[44] J.-K. Bae, M.-C. Park, E.-J. Yang, and D.-W. Seo, "Implementation and performance evaluation for DSRC-Based vehicular communication system," *IEEE Access*, vol. 9, pp. 6878–6887, 2021.
[45] A. Izadi, A. Gholamhosseinian, and J. Seitz, "Modeling and evaluation of the impact of motorcycles mobility on vehicular traffic," *J. Transp. Technol.*, vol. 11, pp. 426–435, 2021.
[46] X. Ma and I. Andréasson, "Estimation of driver reaction time from car-following data: Application in evaluation of general motor–type model," *Transp. Res. Rec.*, vol. 1965, no. 1, pp. 130–141, 2006.
[47] A. N. Gent and J. D. Walter, "The pneumatic tire," National Highway Transportation Safety Administration, DOT HS 810 561, Washington, DC, Feb. 2006.
[48] C. Sommer, R. German, and F. Dressler, "Bidirectionally coupled network and road traffic simulation for improved IVC analysis," *IEEE Trans. Mobile Comput.*, vol. 10, no. 1, pp. 3–15, Jan. 2011.
[49] "OMNet++ discrete event simulator," Nov. 2023. [Online]. Available: https://omnetpp.org/
[50] D. Krajzewicz, J. Erdmann, M. Behrisch, and L. Bieker, "Recent development and applications of SUMO - simulation of urban Mobility," *Int. J. Adv. Syst. Meas.*, vol. 5, no. 3/4, pp. 128–138, 2012.
[51] The National Association of City Transportation Officials, "Signal cycle lengths," Oct. 2023. [Online]. Available: https://nacto.org/publication/urban-street-design-guide/intersection-design-elements/traffic-signals/signal-cycle-lengths/
[52] X. Liu and A. Jaekel, "Congestion control in V2V safety communication: Problem, analysis, approaches," *Electronics*, vol. 8, no. 5, p. 540, May 2019. [Online]. Available: https://www.mdpi.com/2079-9292/8/5/540
[53] A. Autolitano, M. Reineri, R. M. Scopigno, C. Campolo, and A. Molinaro, "Understanding the channel busy ratio metrics for decentralized congestion control in VANETs," in *Proc. Int. Conf. Connected Veh. Expo*, 2014, pp. 717–722.
[54] S. Kuhlmorgen, A. Festag, and G. Fettweis, "Evaluation of multi-hop packet prioritization for decentralized congestion control in VANETs," in *Proc. IEEE Wireless Commun. Netw. Conf.*, 2017, pp. 1–6.

ASHKAN GHOLAMHOSSEINIAN (Member, IEEE) received the bachelor's degree in software engineering from Iran, the master's degree in network engineering from Halmstad University, Halmstad, Sweden, and the Post-master's degree in communications for intelligent transport systems from Eurecom, Biot, France. He is currently working toward the Ph.D. degree in electrical engineering and information technology with Communication Networks Group, Technische Universität Ilmenau, Ilmenau, Germany. His research interests include around intelligent transportation systems and vehicular communications.

JOCHEN SEITZ (Member, IEEE) studied computer science with the University of Karlsruhe, Karlsruhe, Germany. He received the Ph.D. degree in the integration of heterogeneous network management architectures from the University of Karlsruhe, and the Habilitation degree in cooperative network and systems management from the University of Karlsruhe, Karlsruhe. After a Postdoc with Lancaster University, Bailrigg, U.K., working with the Distributed Multimedia Research Group (Prof. Davies). He was a substitute Professor for distributed systems with the University of Technology Braunschweig, Braunschweig, Germany, and since 2001, he has been a Professor for communication networks with the Faculty of Electrical Engineering and Information Technology, Technische Universität Ilmenau, Ilmenau, Germany.